JOURNAL OF Applied Polymer SCIENCE

Effect of Stoichiometry and Cure Prescription on Fluid Ingress in Epoxy Networks

Katherine Frank, Jeffrey Wiggins
School of Polymer and High Performance Materials, University of Southern, Hattiesburg, Mississippi
Correspondence to: J. Wiggins (E-mail: Jeffrey.wiggins@usm.edu)

ABSTRACT: Stoichiometry and cure temperature were evaluated for epoxy systems based on the diglycidyl ethers of bisphenol-A and bisphenol-F and cured with 3,3′- or 4,4′-diaminodiphenylsulfone. The materials were formulated as stoichiometric benchmarks and with an excess of epoxide and cured in two steps (125°C/200°C) or one step (180°C). Dynamic mechanical analysis and free volume testing indicated decreased crosslink density and increased chain packing in the excess-epoxy materials, as well as a narrowing gap in properties between 33- and 44-cured networks with excess epoxy. The narrowing gap was less pronounced in materials cured at 180°C. The excess-epoxy materials were more resistant to water ingress, exhibiting reduced equilibrium water uptake. The excess-epoxy materials were also more resistant to methyl ethyl ketone ingress, which occurred at a slower rate in most excess-epoxy materials. The improvement in fluid resistance was attributed to enhanced chain packing in the materials with lower crosslink densities.

KEYWORDS: crosslinking; structure-property relations; swelling

Received 7 December 2012; accepted 1 February 2013; published online 14 March 2013
DOI: 10.1002/app.39140

INTRODUCTION

Glassy polymer matrix chemistry is an important area of research for advancing fiber-reinforced composite performance. Critical composite properties such as thermal stability, fluid sensitivity, interfacial properties, and deformation characteristics are matrix-dominant. Amine-cured epoxy polymers continue to play a major role in advanced composites due to their high strength, good corrosion resistance, and low shrinkage.

Epoxies formulated with a 1 : 1 ratio of epoxide to amine active hydrogen are considered "stoichiometric" networks. Because epoxy–amine crosslinking is an AA–BB step-growth polymerization, complete conversion is only achieved with 1 : 1 stoichiometry.[2] However, the matrix materials for aerospace-grade epoxies are generally formulated with an excess of epoxy to improve processability and enhance certain properties such as impact strength.[3]. In theory, any deviation from 1 : 1 stoichiometry results in a decrease in crosslink density and an increase in molecular weight between crosslinks and dangling chain ends. This theory has been validated experimentally by several researchers, who measured decreased crosslink density for off-stoichiometry epoxies.[4,5]

In addition to reducing crosslink density, excess epoxy has been shown to alter network architecture by increasing etherification. Etherification occurs when a hydroxyl group reacts with an oxirane ring, creating an ether-based crosslink (as shown in Scheme 1). Etherification has a higher activation energy than epoxy–amine reactions, and therefore, etherification is not considered a competitive reaction unless high temperature and an excess of epoxy are present. The effects of etherification and other stoichiometry-related chemical and architectural variations on fluid resistance are not well understood.

Fluid sensitivity is a critical area of research in epoxy network science, because a high-performance composite structure, such as an aircraft, will be exposed to a number of aggressive fluids during its service life. Examples of aggressive fluids include water, methyl ethyl ketone (MEK), jet fuel, and hydraulic fluids. Exposure to these fluids can precipitate a decrease in key mechanical properties of the matrix.[6–8] Fluid resistance and performance confidence could be improved if the relationships between stoichiometry, network architecture, and solvent susceptibility were fully resolved.

Reports of transport kinetics of small molecules through linear polymer glasses have proliferated in the past 30 years. Diffusion of water through polymeric glasses has been extensively studied and shown to follow classic Fickian behavior, in which uptake rate depends on concentration gradient.[9,10] Fickian diffusion is described by the following equation:

$$\partial\varphi/\partial t = D(\partial^2\varphi/\partial x^2)$$

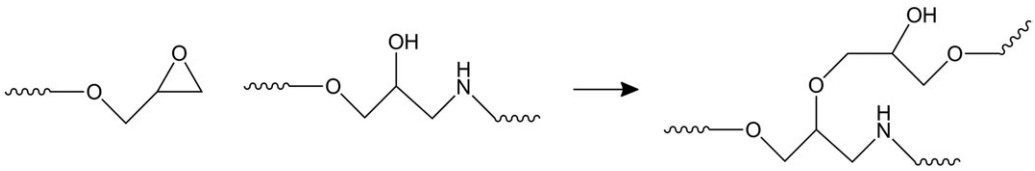

Scheme 1. Ether crosslinking reaction for epoxy.

where φ is the moisture concentration, t is the time, D is the diffusivity, and x is the position.[11]

Moisture diffusion in epoxies has traditionally been analyzed from a chemical affinity perspective, in which water ingress was considered primarily in terms of polarity and hydrogen bonding in the material.[12,13] Recently, researchers have also studied the link between free volume characteristics and water uptake in epoxies.[14–17] Several authors have observed that equilibrium water uptake and water diffusivity decrease with a large excess of epoxide in diglycidyl ether of bisphenol-A (DGEBA)-based systems.[5,18–20] VanLandingham et al. attributed the improvement in water resistance to a two-phase morphology that inhibits water diffusion.[19,21] Research by Halary[5] and Wu et al.[20] posited that decreased crosslink density and improved chain packing are responsible for reduced water uptake observed for excess-epoxy materials. This conclusion is consistent with results from other epoxy research, which suggested that decreased crosslink density in excess-epoxy materials results in lower free volume for those epoxies.[4,22]

Reports on the diffusion of organic solvents through glassy polymers are less common.

Transport of organic solvents through polymer glasses has been shown to follow non-Fickian kinetics; specifically, Case II diffusion is observed.[23] Case II diffusion is defined by linear mass uptake over time due to a constantly moving well-defined flow front, with an unperturbed region of material in the center of the sample persisting until equilibrium. Free volume arguments have been used to successfully explain and predict organic solvent ingress in epoxies.[16,17,24] To the best of our knowledge, no studies have been conducted examining organic solvent diffusion through off-stoichiometry epoxy networks.

The present research evaluates water and organic solvent ingress in a series of aerospace epoxies formulated with a stoichiometric excess of epoxide. Because small excesses of epoxide are often used in industrial processing of epoxy–amine networks, the epoxide excess in this study was limited to 25% in order to provide relevance to real-world conditions. Network architectures were characterized via cure studies, free volume measurements, and dynamic mechanical analysis (DMA), and fluid ingress patterns were correlated to architectural variations.

EXPERIMENTAL

Materials

The following materials were used as received: diglycidyl ether of bisphenol-F (DGEBF, EPON862, EEW = 169, Momentive Specialty Chemicals, Inc., Houston, TX), DGEBA (EPON825, EEW = 177.5, Momentive), 3,3′-diaminodiphenylsulfone (33DDS, Royce International, East Rutherford, NJ, >99% pure, 4 μm particle size), 4,4′-diaminodiphenylsulfone (44DDS, Royce Chemical Corp., >99% pure, 4 μm particle size). Their structures are shown in non-chain-extended form in Scheme 2. Water and MEK were high pressure liquid chromatography (HPLC) grade, supplied by Fisher and used as received for fluid uptake studies.

Formulations

Epoxies were formulated with a 1.25 : 1 molar excess of epoxide to amine active hydrogen. Benchmark epoxies were also made with 1 : 1 stoichiometry. The epoxies were formulated using DGEBA and DGEBF and cured with 33DDS and 44DDS. In a typical reaction, 100.0 g (0.296 mol) DGEBF was charged to a 500 mL Erlenmeyer flask equipped with a vacuum fitting and magnetic stirring device. The epoxide blend was heated to 100°C, and 36.73 g (0.148 mol) 33DDS was added over a 10 min period. Pressure was slowly decreased to $\sim 10^{-3}$ torr, and temperature was increased to 120°C. The mixture was stirred until the amine fully dissolved. At that point, the clear solution was poured into preheated (100°C) silicone test coupon molds of various dimensions. Samples were cured using a two-step prescription (5 h at 125°C and 2 h at 200–225°C) or a one-step prescription (3 h at 180°C). The benchmark and excess-epoxy samples are listed in Table I.

Characterization

Near-Infrared Spectroscopy. The consumption of epoxide groups was followed using near-infrared (IR) spectroscopy in transmission mode. Spectra were recorded using a Thermo Scientific Nicolet 6700 FT-IR in the range of 4000–8000 cm^{-1}. A white light source was used in conjunction with a KBr beam splitter and a deuterated triglycine sulfate (DTGS) detector KBr detector. Samples were prepared by placing uncured resin between glass slides separated by a 0.8 mm Teflon spacer. The reaction progressed in a Simplex Scientific Heating Cell according to a designated curing prescription. Thirty-two scans at 4

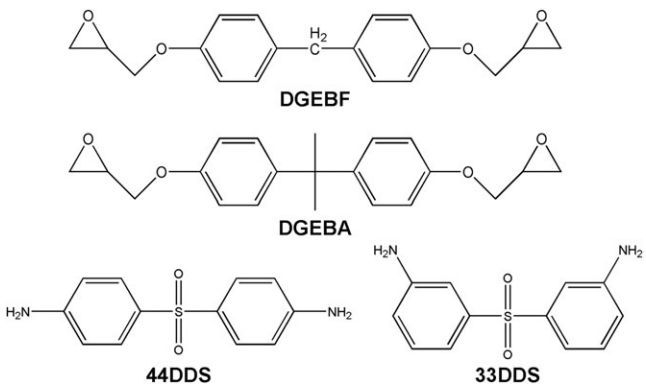

Scheme 2. Epoxy and curative monomers.

Table I. Epoxy Formulations

Sample name	Epoxide (mol)	Curative (mol)	Epoxide (g)	Curative (g)
DGEBF-33	0.296	0.148	100.00	36.73
DGEBF-44	0.296	0.148	100.00	36.73
DGEBA-33	0.282	0.141	100.00	34.97
DGEBA-44	0.282	0.141	100.00	34.97
$DGEBF_{XS}$-33	0.370	0.148	125.00	36.73
$DGEBF_{XS}$-44	0.370	0.148	125.00	36.73
$DGEBA_{XS}$-33	0.352	0.141	125.00	34.97
$DGEBA_{XS}$-44	0.352	0.141	125.00	34.97

cm^{-1} resolution were acquired every 15 min during cure. Epoxide concentration was determined from the peak at 4525 cm^{-1} using the following form of the Beer–Lambert law:

$$A = \varepsilon c l$$

where A is the total absorbance, ε is the molar absorptivity of the functional group in mol kg^{-1} cm^{-1}, c is the concentration of the functional group in kg mol^{-1}, and l is the path length (sample thickness) in cm.[25]

Dynamic Mechanical Analysis. Dynamic mechanical properties, including storage modulus (E') and thermomechanical T_g, were measured with a Thermal Analysis Q800 DMA in tensile mode with a strain amplitude of 0.05% and a frequency of 1 Hz. Temperature was ramped from 50°C to 300°C at a rate of 3°C/min. Crosslink densities were calculated from the rubbery plateau values of E' at T_g +40°C, according to the classical theory of rubber elasticity:

$$\nu = E/(3RT)$$

where ν is crosslink density in mol m^{-3}, E is E' at T_g +40 K, R is 8.314 J mol^{-1} K^{-1}, and T is T_g +40 K.[26]

Positron Annihilation Lifetime Spectroscopy. Positron annihilation lifetime spectroscopy (PALS) was performed on benchmark and excess-epoxy materials cured at 125°C/200°C. Samples for PALS analysis were cast as circular disks with average diameters in the range of 9.5–9.9 mm and thicknesses of ~1–2 mm. Two identical pieces of epoxy sandwiched a 5 μCi ^{22}Na positron source that was sealed between two sheets of 13 μm thick kapton (kapton stops ~5% of the positrons but produces no positronium signal). After wrapping in aluminum foil, this two-sided sample-source arrangement was placed in a small vacuum canister (pumped to ~10^{-2} torr by a mechanical rotary pump). This evacuated source chamber was located between the fast plastic gamma detectors of a typical PALS spectrometer with time resolution of 280 ps. A lifetime spectrum with 4–5 million events was acquired in about 20 h. Standard discrete lifetime fitting showed that only one positronium lifetime in the range 1.6–1.8 ns was required for adequate fitting, and the relative intensity of this positronium component was ~20% for all the samples. The fitted positronium lifetime for each sample was then converted to an average spherical free volume using the well-known Tao–Eldrup model.[27,28]

Fluid Uptake. Fluid uptake studies were conducted using water and MEK. Rectangular epoxy samples having mass of approximately 300 mg and thickness of 1.5 mm were conditioned in a vacuum oven for 12 h at 100°C prior to measuring initial weights. Dry polymer samples were placed in 20 mL scintillation vials containing ~15–18 mL of fluid. The vials were sealed and stored at 25°C in a Fisher Scientific Model 146E incubator. To measure fluid uptake, samples were periodically removed from solution, patted dry, and weighed to the nearest 0.1 mg. Percent change in mass for each sample was calculated as follows:

$$\%\ \text{Change in Mass} = 100 \times (m_w - m_i)/m_i$$

where m_w is the wet mass, and m_i is the initial mass. Four samples were averaged to give each data point.

The Fickian diffusion coefficient (diffusivity, D), which represents a normalized diffusion rate, was calculated from the water uptake curves. At short times diffusivity can be approximated as follows:[29]

$$M_t/M_{\text{inf}} = (4/L) \times (Dt/\pi)^{1/2}$$

where M_t is the water absorption at time t, M_{inf} is the equilibrium water absorption, and L is half the sample thickness in cm (to account for diffusion from both sides), and D is the diffusivity in cm^2 s^{-1}. Diffusivities were calculated from the slopes of the linear regression best-fit lines of plots of M_t/M_{inf} vs. $t^{1/2}$.

RESULTS AND DISCUSSION

The network architecture and fluid resistance of benchmark and excess-epoxy networks were evaluated as a function of chemical composition and cure prescription. Difunctional epoxide monomers (DGEBA and DGEBF) were mixed with aromatic amines (33DDS and 44DDS) and cured with two-step (125°C/200°C) and one-step (180°C) curing prescriptions. The thermoset networks were formulated as stoichiometric benchmarks or with an excess of epoxy.

Excess-epoxy networks were predicted to have different network architectures than their stoichiometric analogues, due to their divergence from the "ideal" step-growth thermoset. This divergence could be evidenced by a decrease in crosslink density and an increase in molecular weight between crosslinks (M_c). The increased presence of dangling chain ends may also affect structure–property relationships in the networks. Excess-epoxy treatments can further alter network architecture by increasing the probability of etherification. Etherification is non-negligible when excess epoxy is present at high temperatures.[30] Etherification increases crosslink density, but the ether-based crosslink is chemically different from the amine-based crosslink that develops from epoxy–amine reactions. In addition to the effect on network backbone, the number of hydroxyl groups differs for the two crosslink structures. Every epoxy–amine reaction generates a new hydroxyl group, whereas the overall number of

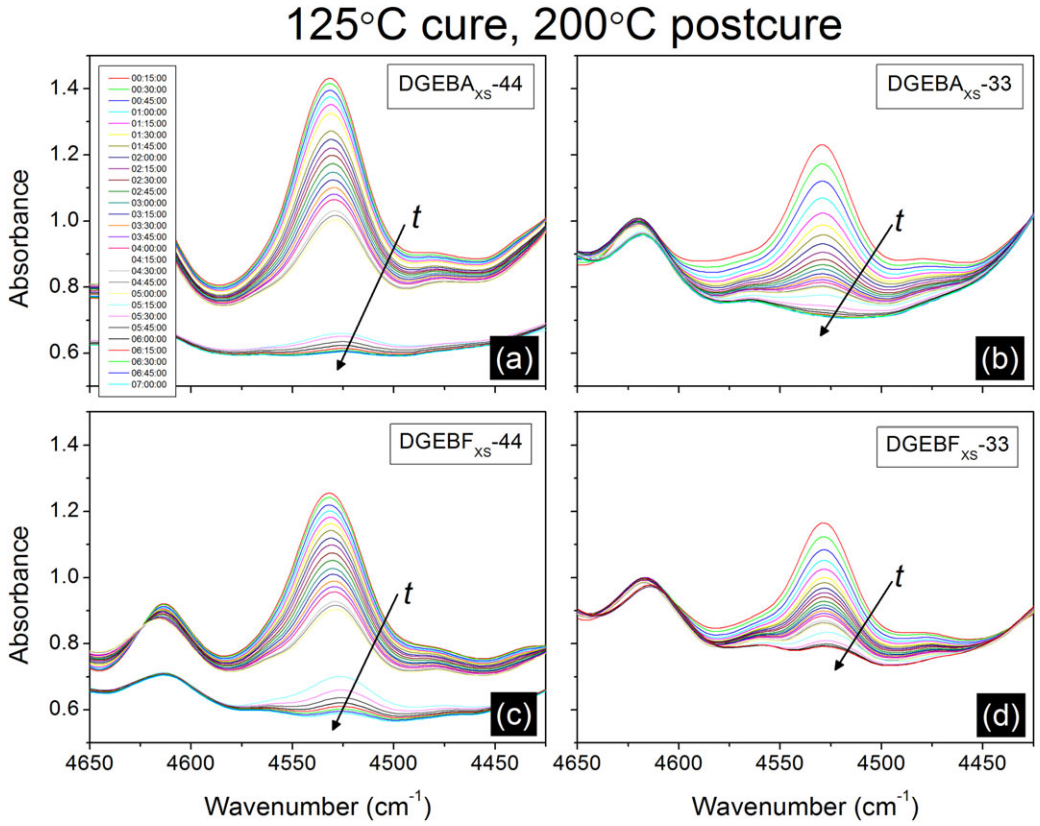

Figure 1. Near-IR peak at 4525 cm^{-1} for epoxies subjected to two-step cure (125°C/200°C): (a) DGEBA$_{XS}$-44, (b) DGEBA$_{XS}$-33, (c) DGEBF$_{XS}$-44, and (d) DGEBF$_{XS}$-33. [Color figure can be viewed in the online issue, which is available at wileyonlinelibrary.com.]

hydroxyls does not change when an etherification reaction occurs. Hydroxyl groups have been associated with increased water ingress due to their ability to hydrogen bond with the water molecule.[19,22]

Architectures of the cured networks were probed via DMA and mechanical testing. Free volume hole sizes (V_h) were determined using PALS. The network was studied through its development using near-IR spectroscopy. The fluid sensitivity of the epoxies was evaluated with MEK and water, and the fluid ingress properties of the materials were correlated to their network architectures.

IR Cure Profiles

The extent of etherification was ascertained using near-IR spectroscopy using the peak at 4525 cm^{-1}, which is associated with the epoxide group. Residual epoxide would be expected for a system in which only epoxy–amine reactions occurred, due to the stoichiometric excess of epoxy. Conversely, a final epoxy concentration below the level predicted by stoichiometry would indicate that etherification reactions occurred. The evolution of the epoxy peak throughout the cure cycle is shown in Figure 1 (two-step cure) and Figure 2 (one-step cure). For most systems, the epoxide peak was reduced to nearly zero by the end of curing. The disappearance of the epoxide peak qualitatively demonstrated etherification for all excess-epoxy materials.

For quantitative evaluation of epoxide concentration ([epox]), the Beer–Lambert Law was employed. Initial [epox] was calculated from epoxide concentration in the neat resin and adjusted for the proportion of resin the epoxy–amine mixture. Projected final [epox] was calculated based on reaction stoichiometry, assuming no etherification reactions. Final [epox] was calculated from the 4525 cm^{-1} peak in the final scan of the cure process. The results of these calculations are listed in Tables II (two-step cure) and III (one-step cure).

All of the excess-epoxy materials except DGEBA$_{XS}$-44 exhibited a lower final [epox] than predicted by the stoichiometric relationship, indicating that etherification reactions occurred. Etherification was more prominent in the epoxies cured at 125°C/200°C. The increased etherification with that cure prescription may be attributed to the postcure step at 200°C, because etherification is more favorable at higher temperatures. The network architecture of the etherified epoxies was presumed to be slightly different from the architecture of benchmark materials, as discussed above.[7] The impact of etherification was considered in the interpretation of PALS, DMA, and fluid uptake results.

PALS Results

Hole sizes of the benchmark and excess-epoxy materials subjected to a two-step cure are listed in Table IV. The benchmark epoxies exhibited a distribution of hole sizes from 67 to 82 Å^3. In the excess-epoxy materials, hole sizes in DGEBA$_{XS}$-33 and DGEBF$_{XS}$-33 decreased slightly and hole sizes in DGEBA$_{XS}$-44 and DGEBF$_{XS}$-44 decreased significantly. Overall, the effect of the excess epoxy on hole size was to reduce all V_hs and to

Applied Polymer SCIENCE

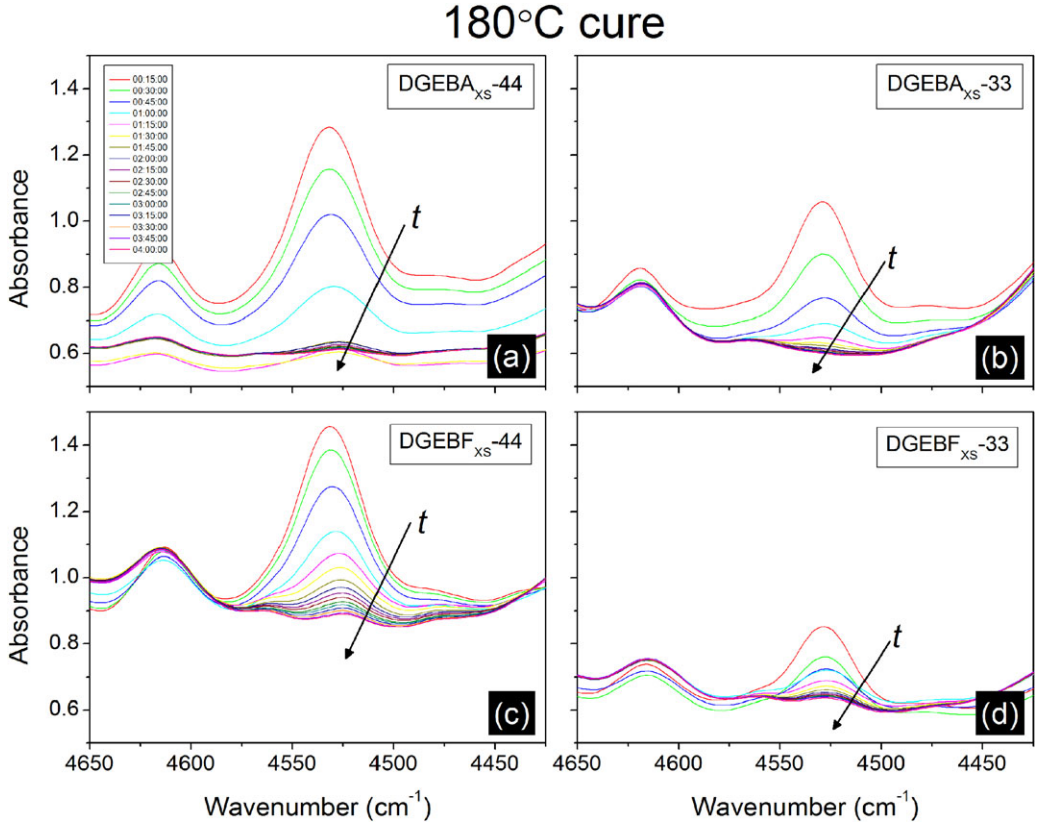

Figure 2. Near-IR peak at 4525 cm^{-1} for epoxies subjected to one-step cure (180°C): (a) DGEBA$_{XS}$-44, (b) DGEBA$_{XS}$-33, (c) DGEBF$_{XS}$-44, and (d) DGEBF$_{XS}$-33. [Color figure can be viewed in the online issue, which is available at wileyonlinelibrary.com.]

reduce V_h difference between 33DDS- and 44DDS-cured epoxies.

The decrease in V_h for all materials may have been due to increased M_c and enhanced chain packing, which could result in smaller hole sizes. The reduced difference in V_h between 33- and 44-cured epoxies suggested increased architectural similarity for the excess-epoxy networks. The difference in V_h between DGEBA-33 and DGEBA-44 (or DGEBF-33 and DGEBF-44) has been attributed to the differences in chain packing efficiency induced by the two isomeric DDS crosslinkers.[16,31] When excess epoxy was used, the DDS segments became a comparatively smaller fraction of the overall network. The epoxide contributed comparatively more of the total network segments in the excess-epoxy materials. Thus, the network architectures of those materials were more similar when the same epoxy resin was used, despite the different amine curatives. Further similarity in the networks may have been induced by etherification, which was more favored under excess-epoxy conditions. The ether crosslink was structurally the same whether 33DDS or 44DDS was used. Therefore, networks with more etherification were more similar regardless of amine isomer. The similarity in network architectures for excess-epoxy materials was confirmed by DMA and fluid uptake results.

DMA Results

Glass transition temperatures (T_g) and crosslink densities (ν) were determined from DMA. DMA curves for the epoxies cured at 125C°/200°C are shown in Figure 3. Two changes in T_g trends were noted. First, a T_g decrease of 15–40°C was recorded for the excess-epoxy materials, compared to benchmarks. Second, the T_g difference between epoxies cured with 33DDS and

Table II. Near-IR Epoxide Concentrations in Epoxies Subjected to Two-Step Cure (125°C/200°C)

System	Initial [epox] (mol kg^{-1})	Proj. final [epox] (mol kg^{-1})	Final [epox] (mol kg^{-1})
DGEBA$_{XS}$-44	4.40	0.88	1.03
DGEBA$_{XS}$-33	4.40	0.88	0.00
DGEBF$_{XS}$-44	4.57	0.91	0.39
DGEBF$_{XS}$-33	4.57	0.91	0.00

Table III. Near-IR Epoxide Concentrations in Epoxies Subjected to One-Step Cure (180°C)

System	Initial [epox] (mol kg^{-1})	Proj. final [epox] (mol kg^{-1})	Final [epox] (mol kg^{-1})
DGEBA$_{XS}$-44	4.40	0.88	0.93
DGEBA$_{XS}$-33	4.40	0.88	0.00
DGEBF$_{XS}$-44	4.57	0.91	0.41
DGEBF$_{XS}$-33	4.57	0.91	0.77

Table IV. PALS for Epoxies Cured at 125°C and Postcured at 200°C

Epoxy system	V_h (Å^3)	Epoxy system	V_h (Å^3)
DGEBF-33	67	$DGEBF_{XS}$-33	64
DGEBF-44	76	$DGEBF_{XS}$-44	64
DGEBA-33	77	$DGEBA_{XS}$-33	76
DGEBA-44	82	$DGEBA_{XS}$-44	73

44DDS narrowed when excess epoxy was used. The T_g difference between DGEBA-33 and DGEBA-44 decreased from 40°C for the stoichiometric materials to 7°C in the excess-epoxy materials ($DGEBA_{XS}$-33 and $DGEBA_{XS}$-44). Likewise, the T_g difference between DGEBF-33 and DGEBF-44 decreased from 22°C for the benchmark networks to 2°C for the excess-epoxy systems ($DGEBF_{XS}$-33 and $DGEBF_{XS}$-44).

The overall drop in T_g can be attributed to the decrease in crosslink density and increase in M_c expected to accompany excess-epoxy formulation. Chain motions were less hindered in the materials with lower crosslink density, enabling the onset of long-range coordinated molecular motion at lower temperatures.

The narrowing gap between T_gs of 33DDS- and 44DDS-cured epoxies mirrors that seen in PALS results. The increased congruency of the excess-epoxy networks was attributed to the relatively higher fraction of epoxy resin and increased role of etherification in those systems.

The decrease in T_g with stoichiometric variation was also observed for the epoxides cured at 180°C (Figure 4). T_g decreased in the excess-epoxy formulations compared to the benchmark materials, due to decreased crosslink density. However, the T_g difference between 33- and 44-cured epoxies did not decrease in the excess-epoxy materials, because the T_g difference was already small in the benchmark epoxies cured at 180°C. According to research by Jackson, when DGEBF or DGEBA were cured at 125°C/200°C, different network architectures were developed with 33DDS and 44DDS curatives due to differences in network growth kinetics. However, when the same epoxies were cured at 180°C, network growth kinetics were similar.[32] Therefore, architectures of the cured networks were similar regardless of curatives, and this similarity was maintained in the excess-epoxy formulations.

The tan δ curves for all DGEBA-based epoxies are shown in Figure 5. The tan δ curves for excess-epoxy DGEBA formulations were similar, regardless of cure temperature or curative. The average T_g of these materials was 158 ± 5°C, compared to 190 ± 20°C for the benchmark DGEBA epoxies. The same trend was present for the DGEBF-based epoxies, shown in Figure 6. The average T_g of the excess-epoxy DGEBF materials was 139 ± 3°C, compared to 164 ± 11°C for the benchmark DGEBF networks. The convergence of tan δ curves suggests that

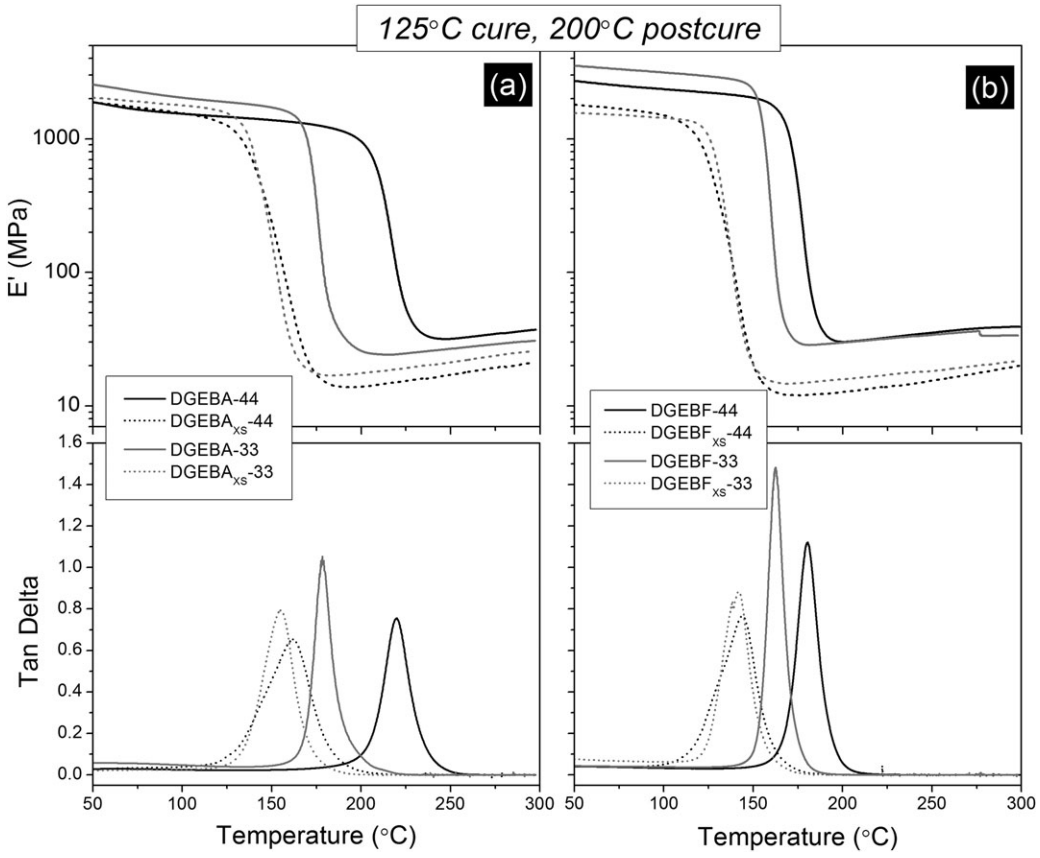

Figure 3. E' and tan δ vs. temperature for (a) DBEGA epoxies and (b) DGEBF epoxies subjected to two-step cure (125°C/200°C).

Applied Polymer SCIENCE

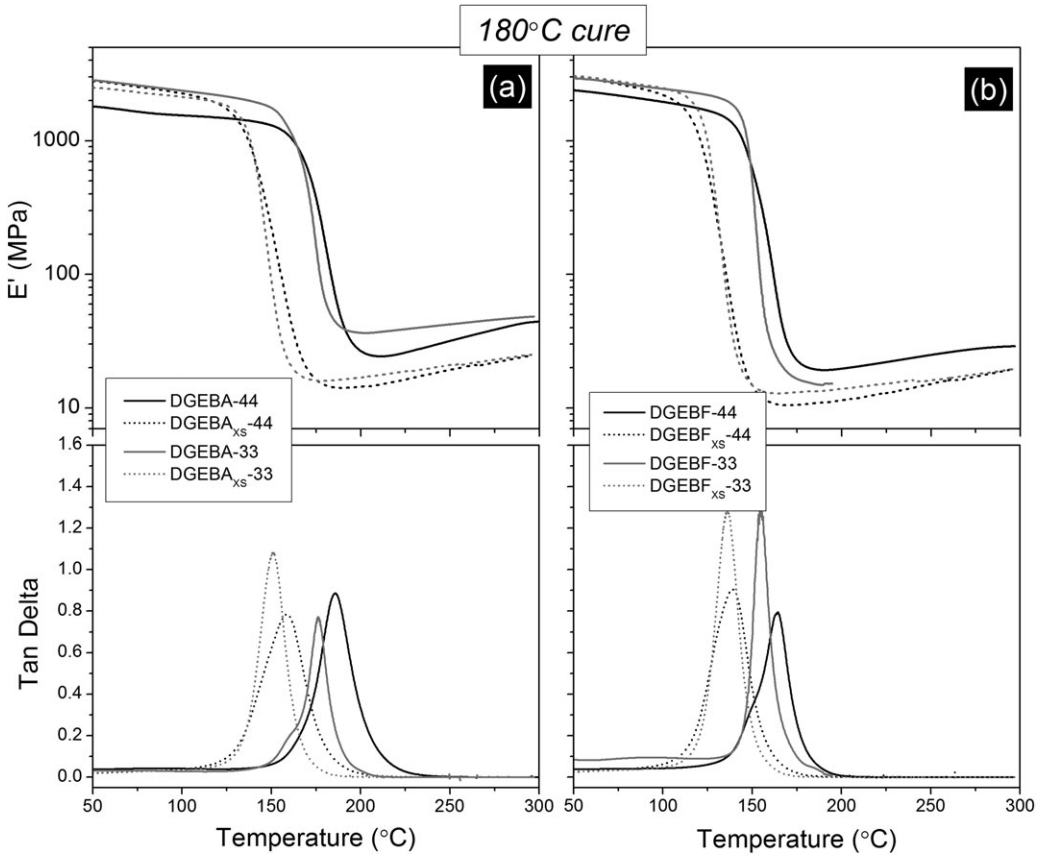

Figure 4. E' and tan δ vs. temperature for (a) DBEGA epoxies and (b) DGEBF epoxies subjected to one-step cure (180°C).

the excess-epoxy networks represent a "limiting case" in architecture and free volume. This limit is established since chain packing cannot be enhanced indefinitely, and the excess-epoxy networks reached the maximum packing efficiency achievable in this family of networks. Excess-epoxy networks cured with different DDS isomers and at different temperatures exhibited the same T_g, because their network architectures had adopted the minimum accessible free volume configuration.

The crosslink densities of the epoxies were calculated using the rubbery plateau values of the storage moduli. For all formulations and cure conditions, crosslink density decreased when excess epoxy was used (Figure 7). This result was consistent with expectations. In a step-growth network, crosslink density is predicted to decrease when the mixture deviates from 1 : 1 stoichiometry, because the reactive group in excess cannot complete crosslinking reactions. Differences in crosslink density between different epoxy formulations also narrowed in the excess-epoxy

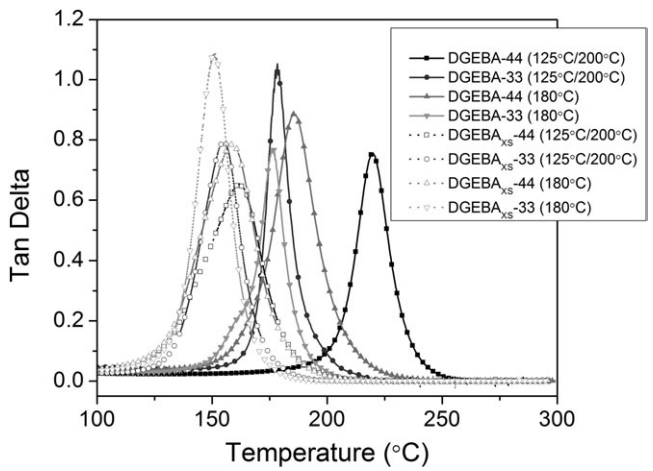

Figure 5. Tan δ vs. temperature for all DGEBA-based epoxies.

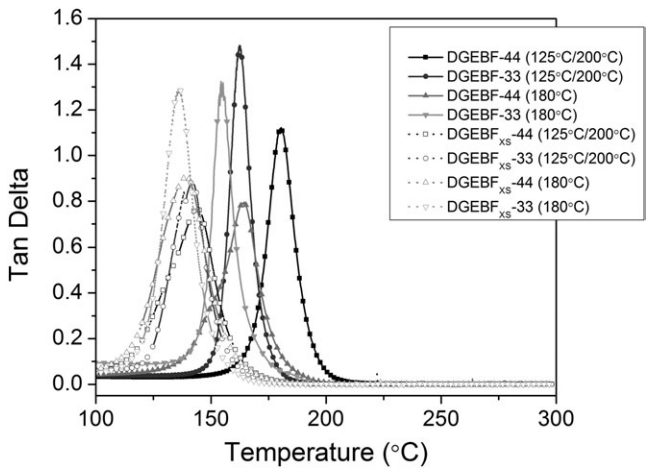

Figure 6. Tan δ vs. temperature for all DGEBF-based epoxies.

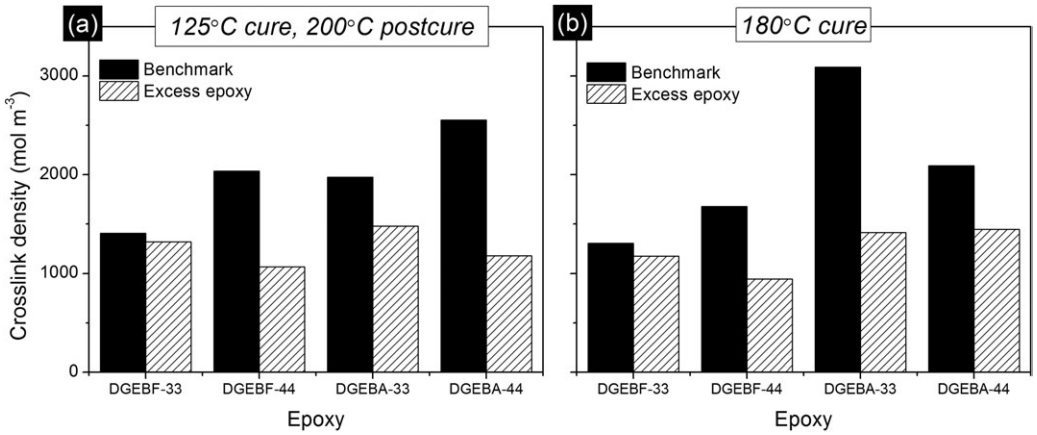

Figure 7. Crosslink densities for (a) epoxies cured at 125°C/200°C and (b) epoxies cured at 180°C.

formulations. The crosslink densities of the benchmark epoxies varied widely, but the crosslink densities of the excess-epoxy networks were similar across curatives and cure conditions.

The crosslink density values for DGEBF-33 epoxies lend support to the "limiting case" argument developed from tan δ curves. Very little change in crosslink density between the excess-epoxy and 1 : 1 formulations was observed for DGEBF-33 for either cure prescriptions. The theory of DGEBF-33 as a limiting case was further substantiated by water and MEK uptake experiments.

Water Uptake Results

Water uptake in the epoxies proceeded according to Fickian diffusion kinetics. For the DGEBA-based materials cured at 125°C/200°C, lower equilibrium uptake was observed for the excess-epoxy samples [Figure 8(a)]. Equilibrium uptake has previously been correlated to fractional free volume (FFV).[14,19] Therefore, the decrease in equilibrium uptake for the excess-epoxy materials suggests a decrease in FFV. FFV likely decreased in those formulations due to enhanced packing of longer, more flexible chain segments. The difference in equilibrium uptake between 33- and 44-cured DGEBA also diminished in the excess-epoxy formulation. The gap decreased from 1.13% for the benchmark epoxies (DGEBA-33 and DGEBA-44) to 0.25% for the excess-epoxy materials ($DGEBA_{XS}$-33 and $DGEBA_{XS}$-44). This data was in good agreement with PALS, T_g, and crosslink density information, which suggested that free volume decreased in the excess-epoxy networks and that the network architectures of 33- and 44-cured DGEBA were more similar in the excess-epoxy formulations.

Slightly different trends were observed for the DGEBF-based epoxies cured at 125°C/200°C [(Figure 8(b)]. Equilibrium water uptake decreased for the $DGEBF_{XS}$-44 epoxy as compared to the benchmark material (DGEBF-44). However, uptake in the $DGEBF_{XS}$-33 epoxy was unchanged compared to DGEBF-33. This data supports the claim that the DGEBF-33DDS benchmark represents the lowest FFV achievable by the epoxies under consideration. $DGEBF_{XS}$-33 did not have substantially lower uptake than DGEBF-33, because the stoichiometric epoxy had already reached maximum packing efficiency and minimum hole size achievable in this family of epoxies. The equilibrium uptake values for all excess-epoxy materials were similar, because they encountered the same limit in packing efficiency.

Trends in water uptake for the materials cured at 180°C were consistent with trends observed for these materials via DMA

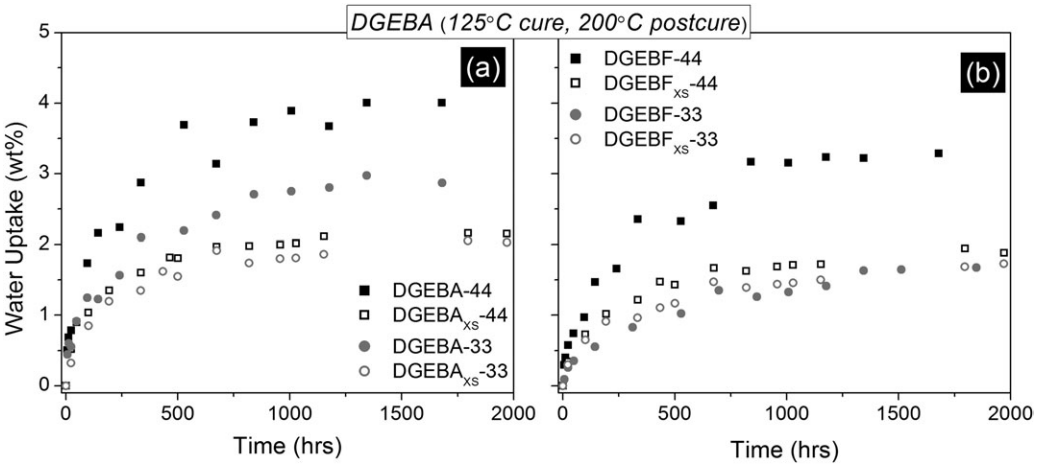

Figure 8. Water uptake vs. time for (a) DGEBA and (b) DGEBF epoxies subjected to two-step cure (125C°/200°C).

Applied Polymer SCIENCE

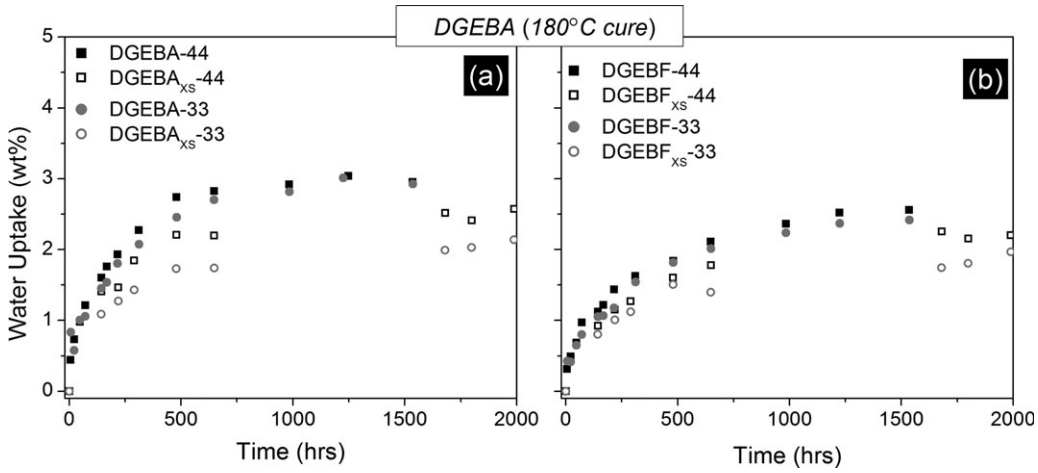

Figure 9. Water uptake vs. time for (a) DGEBA and (b) DGEBF epoxies subjected to one-step cure (180°C).

(Figure 9). The equilibrium uptake was slightly reduced in the excess-epoxy materials as compared to the stoichiometric benchmarks. The equilibrium uptake difference between DGEBA-33 and DGEBA-44 (or DGEBF-33 and DGEBF-44) was narrow in the benchmark materials. The difference, already small, did not decrease substantially with excess-epoxy treatment. Overall, equilibrium uptake for both DGEBA- and DGEBF-based epoxies cured at 180°C was lower than uptake for the same epoxies cured at 125°C/200°C. The lower FFV and V_h of the benchmark epoxies cured at 180°C has already been reported and attributed to enhanced chain packing in the linear-type network growth regime.[32]

Changes in water diffusivity were not as extreme as changes in equilibrium uptake. Diffusivities were calculated from the slope of the best-fit line of M_t/M_{inf} vs. $t^{1/2}$ (Figures 10 and 11), and the values are compared in Figure 12. For most of the materials cured at 125°C/200°C, diffusivities were slightly higher for the excess-epoxy materials. This increase could be due to the lower crosslink densities in those materials, which might hasten water diffusion. For the materials cured at 180°C, diffusivities were slightly lower in the excess-epoxy materials. The 180°C epoxies exhibited less etherification than the 125°C/200°C epoxies, and therefore, they were assumed to have a greater number of unreacted epoxides present in the network as dangling chain ends. The dangling ends may have improved packing efficiency by functioning as antiplasticizers, thereby decreasing D in spite of the lower crosslink density.

In other epoxy systems, an exponential correlation has been noted between diffusivity and V_h.[17] The D–V_h correlation did not have the same slope for the excess-epoxy materials, as illustrated in Figure 13. Diffusivities were higher in the excess-epoxy materials than in stoichiometric epoxies with similar hole sizes. The increased diffusivities may be due to the lower crosslink density, which could facilitate moisture transport through the material. Etherification crosslinks may also be responsible for the increased diffusivities for excess-epoxy materials. Etherification does not generate a new hydroxyl group. Hydroxyl groups may slow diffusion by forming hydrogen bonds with ingressing water molecules. Therefore, a material with a lower hydroxyl concentration may exhibit an increased rate of water diffusion. However, hydroxyl content may have an opposite effect on equilibrium uptake, with equilibrium uptake increasing with hydroxyl content due to affinity between hydroxyls and water.

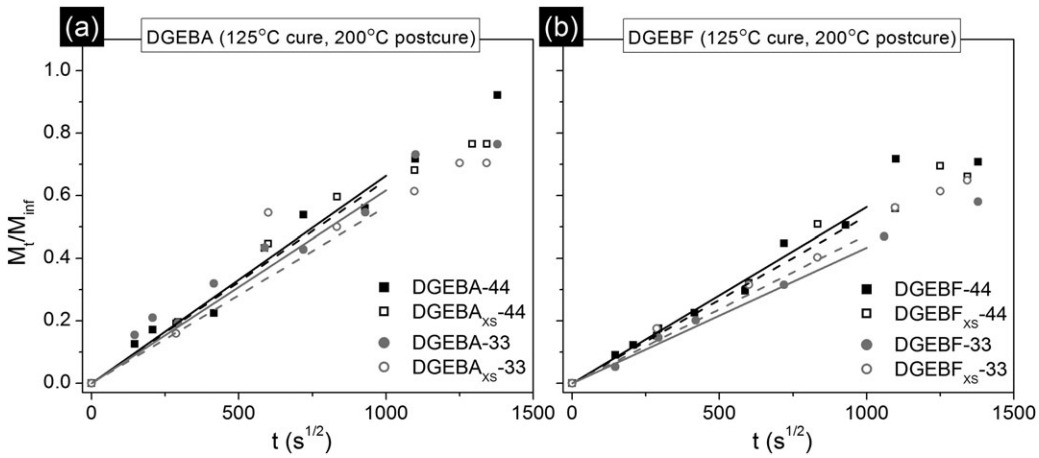

Figure 10. M_t/M_{inf} vs. time $t^{1/2}$ for (a) DGEBA and (b) DGEBF epoxies subjected to two-step cure (125°C/200°C).

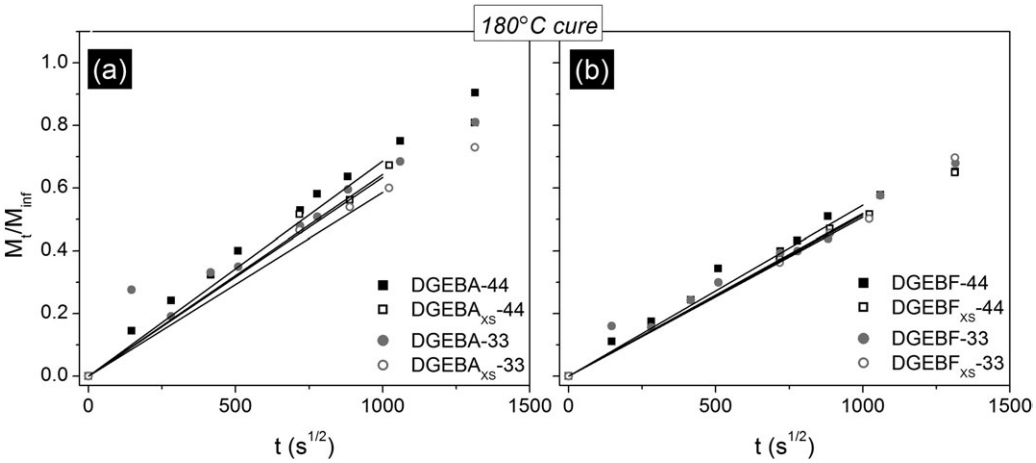

Figure 11. M_t/M_{inf} vs. time $t^{1/2}$ for (a) DGEBA and (b) DGEBF epoxies subjected to one-step cure (180°C).

MEK Uptake Results

MEK uptake was substantially slowed in most excess-epoxy materials, as compared to their stoichiometric analogues. MEK uptake in the excess-epoxy materials cured at 125°C/200°C followed the same general trends as water uptake in those materials. Previous research indicated that uptake rate is higher in DGEBA epoxies than in DGEBF epoxies due to larger hole sizes in the DGEBA materials.[16] For the DGEBA-based epoxies, uptake rate decreased in the excess-epoxy specimens [Figure 14(a)]. For the DGEBF-based epoxies, uptake rate decreased to approximately the rate of the DGEBF-33 epoxy [Figure 14(b)]. For both epoxies, the difference in uptake rate between 33- and 44-cured epoxy was considerably reduced in the excess-epoxy materials.

MEK uptake trends for DGEBA-based epoxies cured at 180°C followed the patterns established by preceding results. MEK uptake rate decreased for the excess-epoxy materials [Figure 15(a)], due to enhanced chain packing in those networks. The gap between DGEBA-33 and DGEBA-44 did not change substantially with excess-epoxy formulation ($DGEBA_{XS}$-33 and $DGEBA_{XS}$-44); the same trend was seen in DMA results for those materials.

MEK uptake trends were less straightforward for the DGEBF materials cured at 180°C. In those materials, MEK uptake rate was near-identical for benchmark and excess-epoxy materials until ~2000 h [Figure 15(b)]. At that time, the uptake curve exhibited a change in slope at ~2000 h that is uncharacteristic of Case II diffusion, and MEK uptake rate became faster for the excess-epoxy materials. The change in diffusion characteristics may be due to the T_g of the $DGEBF_{XS}$ networks. Those networks had the lowest T_gs of any material in this experiment. As a solvent plasticizes the network during Case II diffusion, the T_g of the plasticized region drops considerably.[33] A network with a lower initial T_g will have a lower plasticized T_g. Because the initial T_g of the glassy $DGEBF_{XS}$ networks was low, the T_g onset for plasticized region may have been below 25°C (the temperature at which fluid absorption was conducted). Thus, the diffusion of MEK in $DGEBF_{XS}$-33 and $DGEBF_{XS}$-44 may have shifted from solvent diffusion through a glassy material (pure Case II kinetics) into a regime involving diffusion through rubbery and glassy phases (Case II and Fickian kinetics). A shift in diffusion kinetics near T_g has been demonstrated for other polymer systems.[34,35] After 2000 h, the rubbery region was large enough to influence overall kinetics. Because diffusion through a rubbery material is more facile than diffusion through a glass, MEK uptake rate rose at that point.

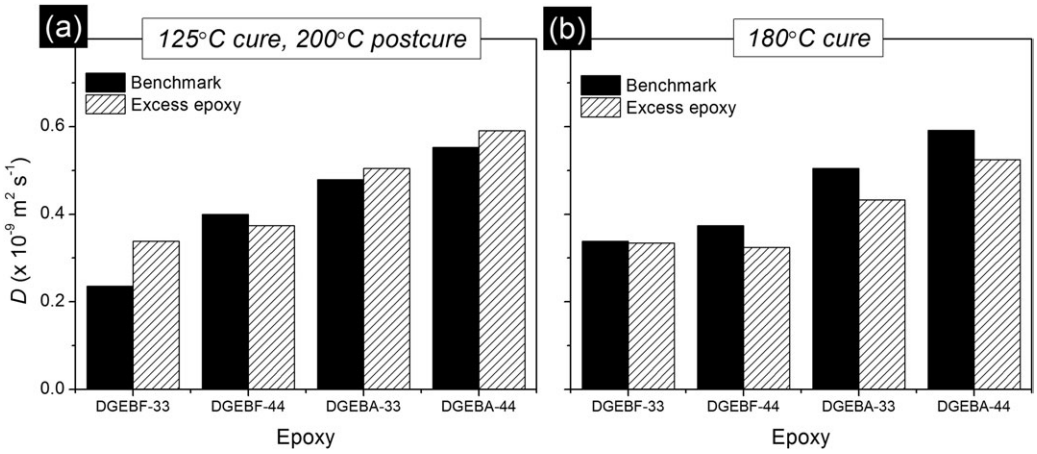

Figure 12. Diffusivity values for (a) epoxies cured at 125°C/200°C and (b) epoxies cured at 180°C.

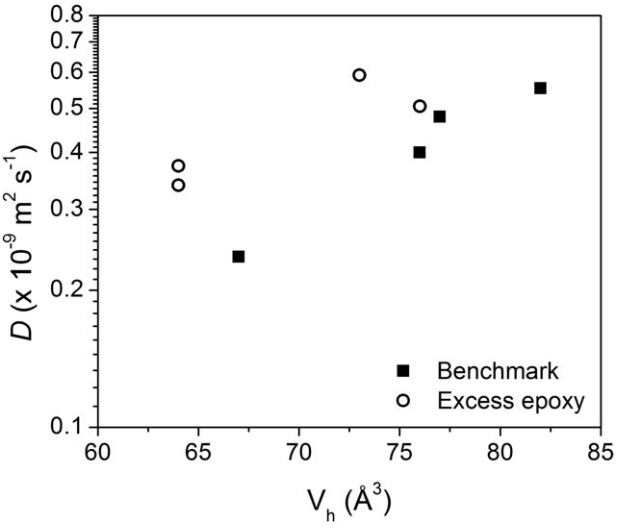

Figure 13. D vs. V_h for epoxies subjected to a two-step cure (125°C/200°C).

Overall, the MEK uptake patterns support the hypothesis that DGEBF-33 represents a "lower limit" for free volume properties and fluid ingress in the epoxy systems under consideration. In some samples, MEK uptake rate was reduced to nearly the level exhibited by DGEBF-33, but no epoxy had slower MEK uptake than that sample. It appears that the DGEBF-33 network assumed the most efficient chain packing achievable in epoxies based on diglycidyl bisphenol ethers and DDS curatives. Other networks came close to this degree of packing efficiency as a result of different stoichiometric and cure conditions, but they but did not exceed it.

CONCLUSIONS

DGEBA and DGEBF were cured with 33DDS and 44DDS in formulations using 1 : 1 and excess-epoxy stoichiometries. Curing was conducted in a two-step (125°C/200°C) or one-step (180°C) process. Cure kinetics were followed via near-IR spectroscopy. IR results indicated that etherification occurred in all systems. Etherification was more prevalent in epoxies cured at 125°C/

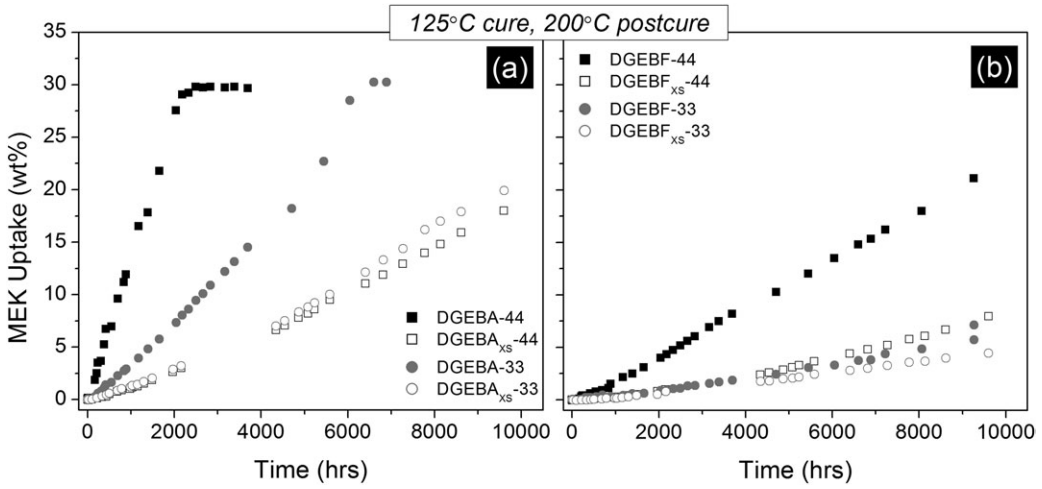

Figure 14. MEK uptake vs. time for (a) DGEBA and (b) DGEBF epoxies subjected to two-step cure (125°C/200°C).

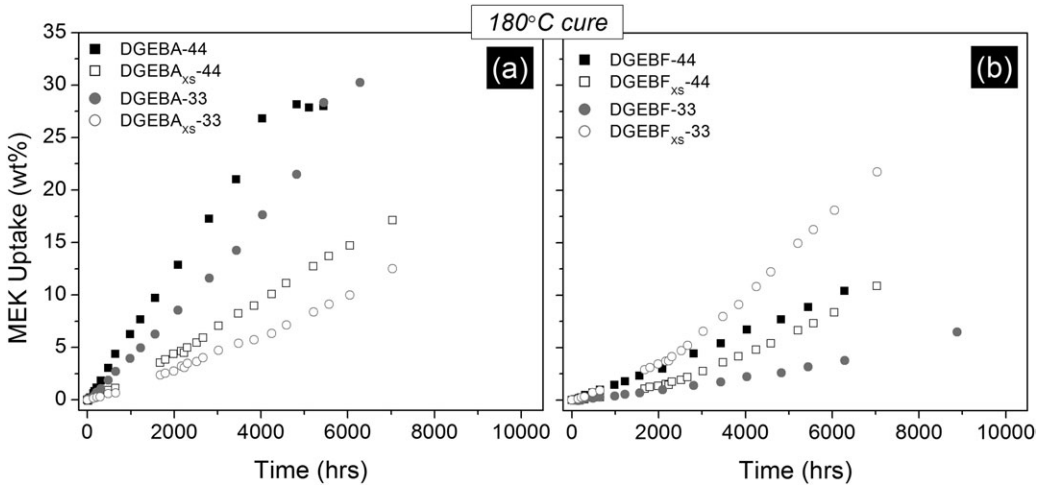

Figure 15. MEK uptake vs. time for (a) DGEBA and (b) DGEBF epoxies subjected to one-step cure (180°C).

200°C due to the high temperature of the postcure. Crosslink density was calculated from the rubbery storage modulus. Crosslink density was reduced in the excess-epoxy formulations, as expected from classical understanding of step-growth networks. The competing effects of etherification, decreased crosslink density, and increased chain packing were responsible for variations in properties exhibited by the materials in this experiment.

Hole sizes were smaller overall for the excess-epoxy materials, and the difference in V_h between 33- and 44-cured materials was reduced. The increasing similarity in the excess-epoxy networks was attributed to increased contributions from etherification crosslinks and the relatively higher fraction of epoxy resin (compared to DDS) in the formulations. The same trend was noted in T_g measurements: T_g decreased in the excess-epoxy materials and the T_g gap between 33- and 44-cured materials narrowed, as compared to stoichiometric benchmarks. The effect on T_g gap was less pronounced in epoxies cured at 180°C, because those networks were already more similar due to similarities in growth kinetics.

Excess-epoxy treatment improved the fluid resistance of the epoxies under consideration. Equilibrium water uptake decreased by as much as 1.7 percentage points in some samples. The reduction in water uptake was attributed to a decrease in FFV, probably due to enhanced chain packing. The gap in equilibrium uptake for 33- and 44-cured materials narrowed, consistent with the narrowing gap in V_h and T_g.

MEK uptake rate decreased for the excess-epoxy formulations. The measured uptake rates were in line with expectations based on enhanced chain packing and etherification, as seen in the water uptake results. Anomalous results were recorded for the $DGEBF_{XS}$ materials, which exhibited a change in diffusion mechanism and an increase in uptake rate as compared to benchmark materials. The change was attributed to the onset of rubbery diffusion in the plasticized region of those networks.

DMA, water uptake and MEK uptake data all provided support for the hypothesis that DGEBF-33 represents a lower limit of free volume achievable in the epoxy systems under consideration. T_g, water uptake rater, water diffusivity, and MEK uptake could not be substantially reduced below the threshold set by DGEBF-33.

The analysis of excess-epoxy materials indicated that the excess-epoxy approach is a viable avenue for improving the fluid resistance of these thermosets. Chain packing and etherification affect network architecture in ways that limit fluid diffusion. However, these architectural changes also resulted in losses in T_g that may not be acceptable in some applications.

ACKNOWLEDGMENTS

The authors thank Prof. David Gidley and Dr. Dhanadeep Dutta at the University of Michigan for PALS experimentation and analysis.

REFERENCES

1. May, C. Epoxy Resins: Chemistry and Technology, 2nd ed.; Marcel Dekker: New York, **1988**.
2. Odian, G. Principles of Polymerization, 4th ed.; John Wiley & Sons: New York, **2004**.
3. Kim, S. L.; Skibo, M. D.; Manson, A. J.; Hertzberg, R. W.; Janiszewski, *J. Polym. Eng. Sci.* **1978**, *18*, 1093.
4. Meyer, F.; Sanz, G.; Eceiza, A.; Mondragon, I. *Polymer* **1995**, *36*, 1407.
5. Halary, J. L. *High Perform. Polym.* **2000**, *12*, 141.
6. Weitsman, Y. J.; Guo, Y. J. *Compos. Sci. Technol.* **2002**, *62* (**6**), 889.
7. Nogueira, P.; Ramirez, C.; Torres, A.; Abad, M. J.; Cano, J.; Lopez, J.; Lopez-Bueno, I.; Barral, L. *J. Appl. Polym. Sci.* **2001**, *80*, 71.
8. Hinkley, J. A.; Connell, J. W. In Long-term Durability of Polymeric Matrix Composites; Pochiraji, K. V., Tandon, G. P., Schoeppner, G. A., Eds.; Springer: New York, **2012**; p 1.
9. Alfrey, T.; Gurnee, E. F.; Lloyd, W. G. *J. Polym. Sci. Pol. Sym.* **1966**, *12*, 249.
10. Chin, J. W.; Nguyen, T.; Aouadi, K. *J. Appl. Polym. Sci.* **1998**, *71*, 483.
11. Crank, J. The Mathematics of Diffusion, 2nd ed.; Clarendon Press: Oxford, **1975**.
12. Zhou, J.; Lucas, J. P. *Polymer* **1999**, *40*, 5505.
13. Mijovic, J.; Zhang, H. *J. Phys. Chem. B.* **2004**, *108*, 2557.
14. Soles, C. L.; Chang, F. T.; Bolan, B. A.; Hristov, H. A.; Gidley, D. W.; Yee, A. F. *J. Polym. Sci. Pol. Phys.* **1998**, *36*, 3035.
15. Soles, C. L.; Yee, A. F. *J. Polym. Sci. Pol. Phys.* **2000**, *38*, 792.
16. Jackson, M.; Kaushik, M.; Nazarekno, S.; Ward, S.; Maskell, R.; Wiggins, J. *Polymer* **2011**, *52*, 4528.
17. Frank, K.; Childers, C.; Dutta, D.; Gidley, D.; Jackson, M.; Ward, S.; Maskell, R.; Wiggins, J. *Polymer* **2012**. doi: 10.1016/j.polymer.2012.11.065.
18. Grave, C.; McEwan, I.; Pethrick, R. A. *J. Appl. Polym. Sci.* **1998**, *69*, 2369.
19. VanLandingham, V. R.; Eduljee, R. F.; Gillespie, J. W. *J. Appl. Polym. Sci.* **1999**, *71*, 787.
20. Wu, L.; Hoa, S. V.; Ton-That, M. *J. Appl. Polym. Sci.* **2006**, *99*, 580.
21. VanLandingham, V. R.; Eduljee, R. F. *J. Appl. Polym. Sci.* **1999**, *71*, 699.
22. Diamant, Y.; Marom, G.; Broutman, L. J. *J. Appl. Polym. Sci.* **1981**, *26*, 3015.
23. Thomas, N. L.; Windle, A. H. *Polymer* **1981**, *22*, 627.
24. Ramesh, N.; Davis, K. P.; Zielinski, J. M.; Danner, R. P.; Duda, J. L. *J. Polym. Sci. Pol. Phys.* **2011**, *49*, 1629.
25. Campbell, D.; Pethrick, R. A.; White, J. R. Polymer Characterization, 2nd ed.; CRC Press: Boca Raton, **2000**.
26. Hiemenz, P. C.; Lodge, T. P. Polymer Chemistry, 2nd ed.; CRC Press: Boca Raton, **2007**.
27. Tao, S. J. *J. Chem. Phys.* **1972**, *56*, 5499.
28. Eldrup, M.; Lightbody, D.; Sherwood, J. *N. Chem. Phys.* **1981**, *63*, 51.
29. Loos, A. C.; Springer, G. S. Environmental Effects on Composite Materials; Technomic: Westport, **1981**.

30. Sohn, D. W.; Ko, K. J. *Korea Polym. J.* **1999**, *7*, 181.
31. Grillet, A. C.; Galy, J.; Gerard, J. F.; Pascault, J. P. *Polymer* **1991**, *32*, 1885.
32. Jackson, M. B. Effects of Molecular Architecture on Fluid Ingress Behavior of Glassy Polymer Networks; Ph.D. Dissertation; University of Southern Mississippi: Hattiesburg, MS, **2011**.
33. Nicolais, L.; Drioli, E.; Hopfenberg, H. B.; Tidone, D. *Polymer* **1977**, *18*, 1137.
34. Ercken, M.; Adriaensens, P.; Reggers, G.; Carleer, R.; Vanderzande, D.; Gelan, J. *Macromolecules* **1996**, *29*, 5671.
35. Doppers, L. M.; Sammonm, C.; Breen, C.; Yarwood, J. *Polymer* **2006**, *47*, 2714.